Subpicosecond photocarrier lifetimes in GaSb/ErSb nanoparticle superlattices at 1.55 μm

M. P. Hanson,[a] D. C. Driscoll, J. D. Zimmerman, and A. C. Gossard
Materials Department, University of California at Santa Barbara, Santa Barbara, California 93106-5050

E. R. Brown
ECE Department, University of California, at Santa Barbara, Santa Barbara, California 93106

(Received 17 May 2004; accepted 16 August 2004)

We demonstrate subpicosecond photocarrier lifetimes at 1.55 μm in GaSb/ErSb nanoparticle superlattices grown by molecular beam epitaxy. Pump–probe measurements were made with a 1.55 μm mode-locked laser in transmission geometry to determine the photocarrier lifetime. The lifetime is found to be dependent on the size of the ErSb particles, amount of ErSb, and the distance between layers of particles. Through manipulation of these three parameters the photocarrier lifetime can be tuned down to less than 300 fs, the temporal limit of our experiment. © *2004 American Institute of Physics*. [DOI: 10.1063/1.1805711]

Materials with subpicosecond photocarrier lifetimes are important for high-speed photodetectors,[1] photomixers,[2] ultrafast photoconductive switches,[3] and THz pulse generators.[4] Low temperature-grown (LTG) GaAs[5] and more recently superlattices of ErAs particles in GaAs[6] have been used successfully for devices operating at wavelengths between ~750 and 850 nm. It has proven more difficult to produce a similar material capable of strongly absorbing at 1.55 μm. LTG InGaAs has not been nearly as effective as LTG GaAs at shortening carrier lifetimes.[7] Fe ion-bombarded InGaAs has been more successful[8] but requires damaging postgrowth treatment, which may limit integration into device structures. InGaAs containing ErAs particles has been shown to have carrier lifetimes around 1 ps.[9,10]

In this letter we present carrier lifetime measurements of a material consisting of layers of semimetallic ErSb nanoparticles within a GaSb matrix grown by molecular beam epitaxy (MBE). We show that by adjusting the amount of ErSb, the size of the ErSb particles, and the spacing of the layers, photocarrier lifetimes can be tuned down to less than 300 fs. Previous work has examined the MBE growth of these superlattices and shown their ability to reduce and tune the as-grown hole concentration in GaSb.[11] Like GaSb, ErSb has a cubic lattice; however, ErSb crystallizes in the rocksalt structure rather than the zinc blende structure of GaSb. The lattice mismatch is less than 0.2%. Surface chemistry, not strain, drives ErSb to grow on GaSb in an island growth mode. By depositing ErSb in amounts less than that required for the islands to coalesce into a complete film, a layer of isolated particles about a nanometer in height is formed. The lateral size and density of these particles is determined by the amount of ErSb deposited. In larger depositions, small particles merge to form larger particles, reducing the density of particles in the layer, while increasing the average particle size. This layer of particles is epitaxially overgrown with GaSb and the process is repeated to form a superlattice. Structures examined in this letter consist of 620-nm-thick superlattices containing layers of ErSb particles separated by GaSb spacer layers. Depositions of ErSb are stated in monolayers (ML) as if the ErSb grew in a layer-by-layer growth mode where 1 ML corresponds to ~3.05 Å of bulk film thickness. In addition to the superlattice samples, a 620-nm-thick layer of GaSb was also grown as a reference sample. All samples were grown by MBE at 530 °C on relaxed 500 nm AlSb buffer layers nucleated on semi-insulating GaAs (100) orientated substrates. A diagram of the sample structure is shown in the inset of Fig. 1.

Pump–probe lifetime measurements were made at a wavelength of 1.55 μm using a commercial femtosecond Er-doped-fiber-based mode-locked laser and fiber-optic components in a transmission geometry. The laser produces a pulse train with a repetition rate of 25 MHz and an average output power of 8.6 mW. We estimate an injected carrier density of $\sim 10^{18}$ cm^{-3}. The pulse train from the laser is split into pump and probe arms via a 20 dB fiber splitter. The −20 dB probe beam runs through a variable delay line with a maximum delay of 300 ps before passing into a fiber-to-free-space coupler which focuses the beam onto the sample. The

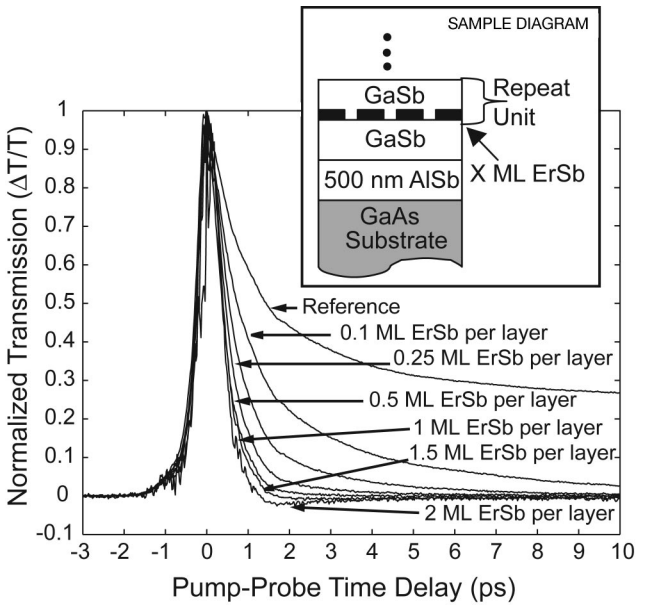

FIG. 1. Normalized differential transmission $\Delta T/T$ plotted against pump–probe delay for various ErSb depositions in a 30 period, 20 nm spacing, ErSb/GaSb superlattice. The inset shows the ErSb/GaSb superlattice structure.

[a]Electronic mail: micah@engineering.ucsb.edu

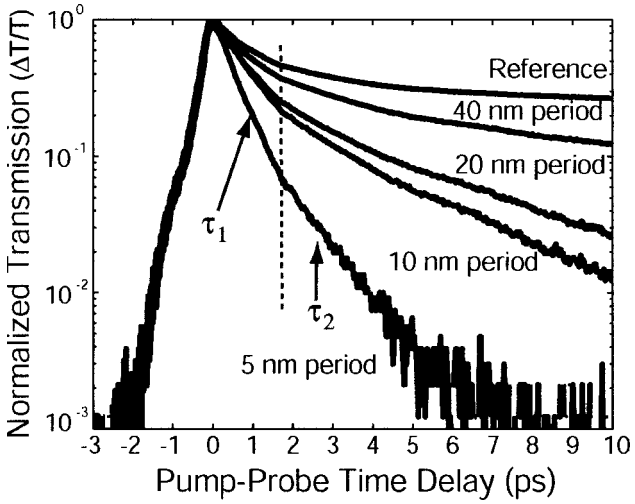

FIG. 2. Normalized differential transmission $\Delta T/T$ plotted against pump–probe delay on a log scale for various layer spacings in a 620-nm-thick ErSb/GaSb superlattice containing 0.1 ML of ErSb per layer. The number of periods was adjusted to maintain a constant thickness thereby increasing the 3D density of ErSb particles. The section of the plot fitted to obtain τ_1 is approximately on the left side of the dashed line, while the portion fitted to obtain τ_2 is on the right.

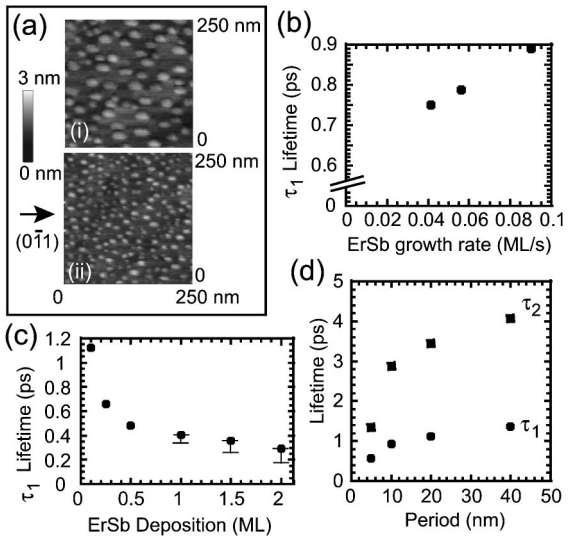

FIG. 3. (a) Atomic force microscopy image of a 0.75 ML deposition of uncovered ErSb islands on a GaSb surface grown at (i) 0.04 ML/s and (ii) 0.09 ML/s. (b) The calculated lifetime τ_1 (ps) is plotted against ErSb growth rate for ~0.5 ML ErSb deposition per layer in a 30 period, 20-nm spacing, ErSb/GaSb superlattice. (c) The calculated lifetime τ_1 (ps) is plotted against ErSb deposition per layer in a 30 period, 20nm spacing, ErSb/GaSb superlattice. Estimated error bars are shown for lifetimes near the experimental limit. (d) The calculated lifetimes, τ_1 and τ_2, are plotted against period spacing in a 620-nm-thick ErSb/GaSb superlattice containing 0.1 ML of ErSb per layer.

pump beam passes through a "U-bench" containing a mechanical chopper before being focused onto the sample via a second fiber-to-free-space coupler. The probe beam signal is collected by an InGaAs photodetector connected to a lock-in amplifier. The rise time of the leading edge of the cross-correlation measurement is ~300 fs, which is the temporal limit of the experiment. Lifetimes were obtained by fitting the portion of the tail between 90% and 10% of the signal peak to an exponential expression $I_0 \exp(-t/\tau)$, where τ is the photocarrier lifetime. In samples exhibiting longer tails, evidence of a secondary recombination mechanism was observed. In these cases the data are better fit with the sum of two exponentials. In these cases one lifetime τ_1 represents the fast initial decay and the other τ_2 represents the slower secondary recombination. Further details of the experimental setup have previously been published.[10]

Three sets of ErSb containing samples were studied. In the first set, the period of the superlattice was kept constant at 20 nm, and the ErSb deposition per layer was changed. In this set, depositions between 0.1 and 2 ML per layer were examined. Figure 1 shows the normalized differential transmission on a linear scale for these samples along with the reference sample. All ErSb containing samples show a faster decay than the reference GaSb layer. As shown in Fig. 3(c), when the deposition of ErSb per layer is increased, the photocarrier lifetime is decreased. For the 2 ML case the rise time is approximately equal to the fall time indicating a maximum upper bound on the photocarrier lifetime of ~300 fs. For samples with greater than 0.5 ML of ErSb no evidence of secondary recombination, τ_2, was observed.

In the second set of samples the ErSb deposition was kept constant at 0.1 ML and the spacing between layers was varied from 5 to 40 nm. The number of periods was adjusted to maintain a constant active layer thickness of 620 nm. Figure 2 shows the normalized differential transmission on a log scale for these samples along with the reference sample. These samples show evidence of a slower secondary recombination mechanism indicated by the change in slope that occurs just prior to 2 ps of delay. As the thickness between ErSb layers is decreased, both the initial decay, represented by τ_1, and the secondary decay, represented by τ_2, decrease. This trend is illustrated in Fig. 3(d), which shows τ_1 and τ_2 plotted as a function of layer spacing.

In order to separate the effects due to the total amount of ErSb in the sample, the ErSb particle size, and the distance between layers of particles, three samples were grown using different ErSb growth rates but maintaining the same period and ErSb deposition. In this way the particle size is changed, but the total amount of ErSb in the layer and throughout the structure is the same. Figure 3(a) shows atomic force microscopy images of two samples with uncovered 0.75 ML ErSb depositions. The top image (i) shows a sample grown at a rate of 0.04 ML/s, and the bottom image (ii) shows a sample grown at a rate of 0.09 ML/s. The faster growth rate forms a higher density of smaller particles while the slower growth rate forms a layer of larger more sparsely distributed particles. For the same ErSb deposition and superlattice period it is observed that samples grown with lower growth rates, and therefore larger ErSb particles, have shorter lifetimes. Figure 3(b) shows a plot of lifetime versus growth rate for a deposition of approximately 0.5 ML per layer in a 20 nm period superlattice.

Table I shows a summary of the photocarrier lifetimes and transport properties obtained from Hall measurements of the samples discussed in this letter. The reference sample has the highest free hole concentration and the longest lifetime, exceeding 30 ps. The actual reference sample lifetime was not extracted due to the long time scale and nonexponential nature of the decay. The addition of ErSb reduces the lifetime. As shown in Table I the lifetime depends monotonically on the ErSb deposition (a), the superlattice period (b), and the ErSb growth rate (c). The lifetime decreases for higher depositions, shorter superlattice periods, and slower growth rates. Both higher ErSb depositions and slower ErSb

TABLE I. Room temperature electrical properties and photocarrier lifetimes for various (a) ErSb depositions (Dep) in a 30 period, 20 nm spacing, ErSb/GaSb superlattice, (b) period spacings in a 620-nm-thick ErSb/GaSb superlattice containing 0.1 ML of ErSb per layer, and (c) ErSb growth rates for a ~0.5 ML deposition of ErSb in a 30 period, 20nm spacing, ErSb/GaSb superlattice.

(a)	Dep (ML)	p (cm^{-3})	Mobility ($cm^2/V\ s$)	Resistivity (Ω cm)	Lifetime (ps) τ_1	Lifetime (ps) τ_2
	Ref.	3.3×10^{16}	577	0.34	>30	>30
	2	1.8×10^{16}	166	2.13	0.29	···
	1.5	1.5×10^{16}	171	2.53	0.36	···
	1	1.0×10^{16}	191	3.24	0.40	···
	0.5	3.4×10^{15}	205	9.23	0.48	1.58
	0.25	3.1×10^{15}	260	7.91	0.66	2.58
	0.1	3.1×10^{15}	297	7.05	1.12	3.44

(b)	Period (nm)	p (cm^{-3})	Mobility ($cm^2/V\ s$)	Resistivity (Ω cm)	Lifetime (ps) τ_1	Lifetime (ps) τ_2
	40	8.1×10^{15}	346	2.24	1.37	4.08
	20	3.1×10^{15}	297	7.05	1.12	3.44
	10	1.0×10^{15}	314	19.5	0.92	2.88
	5	8.2×10^{14}	235	32.6	0.57	1.34

(c)	GR (ML/s)	p (cm^{-3})	Mobility ($cm^2/V\ s$)	Resistivity (Ω cm)	Lifetime (ps) τ_1	Lifetime (ps) τ_2
	0.09	2.9×10^{15}	196	10.8	0.89	2.31
	0.056	2.8×10^{15}	236	9.40	0.79	2.32
	0.04	3.7×10^{15}	222	7.63	0.75	2.18

growth rates lead to larger ErSb particles, resulting in a consistent trend of shorter lifetimes for larger ErSb particles. The experimental data suggest that the reduction of lifetime is primarily due to trap states introduced by ErSb particles rather than the change in free hole concentration. Note the opposite trends of lifetime and free hole concentrations in Tables I(a) and I(b). This is not unexpected because the optically injected carrier density ($\sim10^{18}$ cm^{-3}) is significantly higher than the equilibrium hole concentration (10^{15}–10^{16} cm^{-3}).

The lifetime depends sublinearly on the superlattice period [Table I(b) and Fig. 3(c)] which differs from the ErAs/GaAs system. In the ErAs/GaAs system a quadratic dependence, attributed to diffusion-limited lifetimes, has been observed by both time-resolved photoreflectance[6] and photoconduction.[9] It should be noted that both of these studies examined the period dependence of superlattices containing much larger ErAs particles, with depositions of ~1 ML. This may account for some of the deviation but more experimentation is required. A simple Shockley–Read–Hall model cannot explain the sublinear dependence in the ErSb/GaSb system either; reducing the superlattice period, L, increases the density of traps per unit volume, N_t. Therefore if the recombination process obeyed a simple Shockley–Read–Hall relationship, in which the trap density is the limiting factor, one would expect a linear increase with period since $\tau \propto 1/N_t \propto L$.

The carrier lifetime trends observed in these experiments could be explained by deviations in the band structure of small ErSb particles from that of the bulk. As the size of ErSb particles is reduced, the ErSb particles may exhibit a semimetal to semiconductor transition as the particles become less bulk-like and more atomic-like. This transition has been predicted[12] and observed[13] in similar materials. The secondary recombination observed in smaller ErSb depositions could be a result of this phenomenon. Since the recombination rate decreases with increasing band gap, the emergence of a band gap in small ErSb particles would lead to an increase in the intraparticle electron–hole recombination rate. In this case one would expect a fast initial decay in the differential transmission as electrons and holes are captured by the ErSb particles. However, further capture of electrons and holes would be limited by the time required for electrons and holes to recombine within the particle. This would explain the observed change in the differential transmission decay for small ErSb depositions. Furthermore, as the particle size is reduced the band gap is expected to increase which should increase the intraparticle recombination time. Thus samples containing smaller particles should, as observed in Table I, exhibit longer lifetimes and two-step recombination. Further experimentation and band structure theory is required to prove this speculation.

In conclusion, we have demonstrated subpicosecond photocarrier lifetimes at 1.55 μm as short as 300 fs. This is a conservative estimate since we are limited by the pulsewidth of the pump laser in our experimental setup. The lifetimes can be tuned by adjusting growth parameters such as ErSb deposition, ErSb growth rate, and superlattice period. The hole concentrations in the materials with the shortest lifetimes are still too high for optimum performance of photomixers and high-speed photodetectors. Use of larger depositions at slower growth rates, spaced closer together, could result in both very short lifetimes and the higher resistances required for improved photodetectors and photomixers operating at 1.55 μm.

This work was supported by the Office of Naval Research. The authors would like to thank Herb Kroemer and Christoph Kadow for useful discussions.

[1] Y. Chen, S. Williamson, T. Brock, F. W. Smith, and A. R. Calawa, Appl. Phys. Lett. **59**, 1984 (1991).
[2] E. R. Brown, F. W. Smith, and K. A. McIntosh, J. Appl. Phys. **73**, 1480 (1993).
[3] S. Gupta, M. Y. Frankel, J. A. Valdmanis, J. F. Whitaker, G. A. Mourou, F. W. Smith, and A. R. Calawa, Appl. Phys. Lett. **59**, 3276 (1991).
[4] Y. C. Shen, P. C. Upadhya, E. H. Linfield, H. E. Beere, and A. G. Davies, J. Appl. Phys. **83**, 3117 (2003).
[5] F. W. Smith, H. Q. Le, V. Diadiuk, M. A. Hollis, A. R. Calawa, S. Gupta, M. Frankel, D. R. Dykaar, G. A. Mourou, and T. Y. Hsiang, Appl. Phys. Lett. **54**, 890 (1989).
[6] C. Kadow, A. W. Jackson, A. C. Gossard, J. E. Bowers, S. Matsuura, and G. A. Blake, Physica E (Amsterdam) **7**, 3510 (2000).
[7] S. Gupta, J. F. Whitaker, and G. A. Mourou, IEEE J. Quantum Electron. **28**, 2464 (1992).
[8] C. Carmody, H. H. Tan, C. Jagadish, A. Gaarder, and S. Marcinkevicius, Appl. Phys. Lett. **82**, 3913 (2003).
[9] M. Griebel, J. H. Smet, D. C. Driscoll, J. Kuhl, C. Alvarez Diaz, N. Freytag, C. Kadow, A. C. Gossard, and K. von Klitzing, Nat. Mater. **2**, 122 (2003).
[10] M. Sukhotin, E. R. Brown, D. Driscoll, M. Hanson, and A. C. Gossard, Appl. Phys. Lett. **83**, 3921 (2003).
[11] M. P. Hanson, D. C. Driscoll, C. Kadow, and A. C. Gossard, Appl. Phys. Lett. **84**, 221 (2004).
[12] S. J. Allen, Jr., N. Tabatabaie, C. J. Palmstrom, S. Mounier, G. W. Hull, T. Sands, F. DeRosa, H. L. Gilchrist, and K. C. Garrison, Surf. Sci. **228**, 13 (1990).
[13] L. Bolotov, T. Tsuchiya, A. Nakamura, T. Ito, Y. Fujiwara, and Y. Takeda, Phys. Rev. B **59**, 12236 (1999).